Electron-paramagnetic-resonance identification of a trigonal chromium-indium pair in silicon

P. Emanuelsson, P. Omling, and H. G. Grimmeiss
Department of Solid State Physics, University of Lund, Box 118, S-221 00 Lund, Sweden

J. Kreissl and W. Gehlhoff
Academy of Sciences, Centre for Scientific Instruments, Rudower Chaussee 6, Berlin 1199, Federal Republic of Germany

(Received 27 March 1991)

An EPR spectrum in silicon doped with chromium and indium is reported. The spectrum, which shows a complicated fine and hyperfine structure could be identified as originating in a chromium-indium pair of trigonal symmetry. The fine structure corresponds to transitions within the $^6S_{5/2}$ ground manifold of the trigonal distorted Cr^+ ion and is rather complicated because the zero-field splitting and the Zeeman energies are of comparable magnitudes. For the hyperfine structure, the indium quadrupole interaction was found to play an important role. Both the fine and hyperfine structure could be successfully explained using a computer diagonalization of the corresponding spin Hamiltonian. The experimental results are consistent with a pair model of a substitutional In^- with a Cr^+ on a nearest interstitial position.

I. INTRODUCTION

A great number of studies have been made on pairs between transition metals (TM's) and group-III acceptors (A) in silicon. These defects consist of the acceptor on a substitutional site and the TM atom on the nearest-neighbor (NN) or next-nearest-neighbor (NNN) interstitial position. Electron paramagnetic resonance (EPR) has shown to be one of the most powerful tools for investigating these pairs. One of the advantages of this technique is that it can distinguish between different configurations. The NN configuration has trigonal symmetry and the NNN configuration has orthorhombic symmetry, and this is easily determined in an EPR experiment. The first EPR investigation on the TM-acceptor pairs was the comprehensive work of Ludwig and Woodbury in 1962,[1] where they reported EPR spectra of several different Fe-, Mn-, and Cr-acceptor pairs.

In recent years the Fe-acceptor pairs have been studied in detail, and it has been shown that the Fe-Al,[2-4] Fe-Ga[4,5] and Fe-In (Refs. 5–7) pairs can exist in both the NN and NNN configurations, i.e., one of the configurations is metastable. The Mn-acceptor pairs have also been thoroughly investigated,[8-10] but in these cases only the trigonal configuration has been detected.

In the case of Cr-acceptor pairs, three of them (Cr-B, Cr-Al, and Cr-Ga) were reported by Ludwig and Woodbury,[1] all of them revealing trigonal symmetry, i.e., only the NN configuration was observed. They have also been studied in experiments using other techniques. Lemke determined the energy level position for the Cr-B, Cr-Al, and Cr-Ga pairs using space charge techniques,[11,12] while Feichtinger *et al.* performed combined EPR and Hall effect measurements to determine them for the Cr-Al and Cr-Ga pairs.[13] Luminescence spectra which are attributed to the Cr-B and Cr-Ga defects are also reported.[14,15] Cr-In pairs have been observed in two different trigonal configurations using perturbed angular correlation spectroscopy.[16] The EPR spectra reported on Cr-acceptor pairs are, however, not analyzed in detail and the Cr-In pair has not been observed in EPR. There is, therefore, a need of further investigations of these defects.

In this paper we present an EPR spectrum that we identify as originating in a Cr-In pair. The analysis shows that the spectrum corresponds to transitions within the ground-state manifold of the Cr^+ ion in a tetrahedral crystal field distorted by the associated In^- ion.

II. EXPERIMENTAL DETAILS

The samples were prepared from a Czochralski-grown indium-doped (2 Ω cm) silicon crystal. The crystal was oriented and $2\times2\times10$ mm^3 pieces were cut with the long axis in a ⟨110⟩ direction. The pieces were scratched with a wire of chromium and placed in evacuated ampules. The ampules were filled with argon gas, heat treated at 1200 °C for 2 h, and rapidly quenched. In the case of isotope doping a piece of ^{53}Cr was placed next to the silicon crystal in the ampule.

The EPR measurements were performed using a Bruker ESP 300 spectrometer equipped with a helium-gas-flow cryostat, and a ZWG ERS 230 spectrometer equipped with a hydrogen cryostat. In both spectrometers it was possible to illuminate the samples *in situ*.

III. EXPERIMENTAL RESULTS AND ANALYSIS

As a result of iron contamination, the well-known EPR spectra of iron-indium pairs in silicon appeared after the quench.[1,4,6] Also present was the signal corresponding to interstitial chromium.[1] However, when illuminating the sample a new EPR spectrum emerged. This spectrum is shown in the three main directions (⟨100⟩, ⟨111⟩, and ⟨110⟩) in Fig. 1. In the ⟨111⟩ direction some of the lines show a clear hyperfine splitting in ten lines, see Fig.

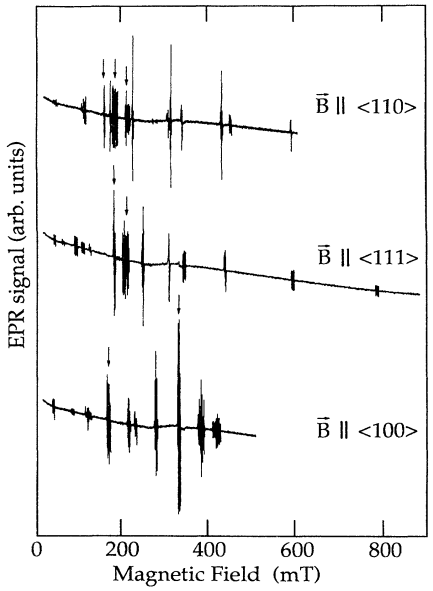

FIG. 1. EPR spectra for the (Cr^+-In^-) pair for the three main directions. The measurements were performed at $T=35$ K and the microwave frequency was 9.526 GHz. The part of the spectrum which is marked is caused by the Fe-In pair.

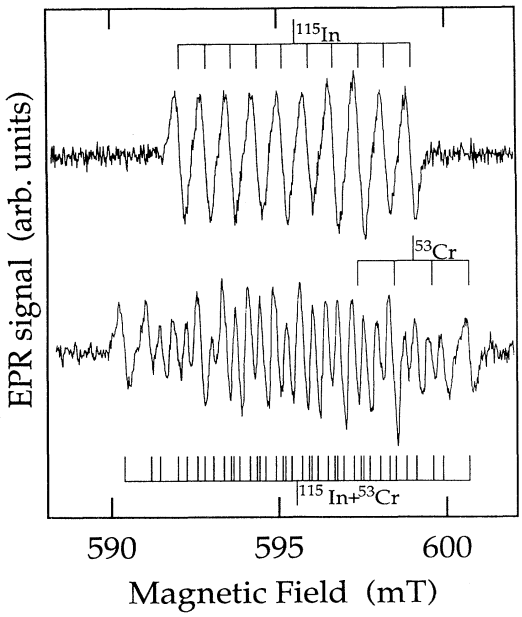

FIG. 2. Hyperfine structure of the electronic spin transition $M=-\frac{3}{2}$ to $M=-\frac{1}{2}$ at $\theta=0°$ for a sample doped with indium and normal chromium (top) or ^{53}Cr (bottom). Also shown is the calculated hyperfine structure caused by ^{115}In ($I=\frac{9}{2}$), ^{53}Cr ($I=\frac{3}{2}$), and by both of them together.

2, proving the existence of one indium atom in the defect. Indium consists of two isotopes, 4.3% ^{113}In and 95.7% ^{115}In, which both have nuclear spin I equal to $\frac{9}{2}$. Since the ratio of the nuclear g values is almost unity, and also since the natural abundance is much greater for one of them, only one set of ten lines is observed. Natural chromium consists to 90.45% of isotopes with $I=0$ and only to 9.55% of the isotope ^{53}Cr with $I=\frac{3}{2}$, i.e., considering the relatively bad signal-to-noise ratio in our measurements no hyperfine structure is expected from a possible chromium atom in the defect. We therefore performed isotope doping with ^{53}Cr, which resulted in a further splitting of each line into four components (see Fig. 2). It is thereby concluded that the defect responsible for the spectrum is a chromium-indium pair. The argumentation above is dependent on the fact that only the allowed hyperfine transitions ($\Delta m=0$) are of importance and, as will be shown below, this is actually the case in this particular direction.

The experimentally determined angular dependence of the spin transitions is plotted as open circles in Fig. 3. Here the hyperfine structure is not included, i.e., the line position is representing the center of gravity of the hyperfine structure. From the complicated pattern shown in Fig. 3, it is no easy matter to determine the symmetry and spin of the system. However, in analogy with the other Cr-acceptor pairs we expect the Cr-In pair to have spin S equal to $\frac{5}{2}$ and trigonal symmetry.[1] Neglecting the hyperfine structure, the spin Hamiltonian (SH) of such a system can be written as follows:

$$H=H_{FS}+H_Z\ , \tag{1}$$

$$H_{FS}=D[S_z^2-1/3S(S+1)]-[(a-F)/180][35S_z^4-30S(S+1)S_z^2+25S_z^2+3S^2(S+1)^2-6S(S+1)]$$
$$+(\sqrt{2}/36)a[S_z(S_+^3+S_-^3)+(S_+^3+S_-^3)S_z]\ , \tag{2}$$

$$H_Z=g_{\parallel}\mu_B B_z S_z+g_{\perp}\mu_B(B_x S_x+B_y S_y)\ , \tag{3}$$

where the symbols have their usual meaning. The z axis coincides with the pair axis, and the x and y axes are chosen according to Ref. 10. When the magnetic field (B) is parallel with the z direction we can get an analytical solution of the energy eigenvalues as a function of the magnetic field. Calling the eigenvalues of S_z for M and inserting the value of the spin, $S=\frac{5}{2}$ we achieve

$$E(\pm M)=\left\{\left[\frac{D}{3}-\frac{(a-F)}{2}\right](|M|-\tfrac{3}{2})+\left[\left[3D+\frac{(a-F)}{6}+\tfrac{3}{2}G[\pm M-(\pm\tfrac{3}{2})]\right]^2+\frac{20a^2}{9}\right]^{1/2}\right\}(|M|-\tfrac{3}{2})$$
$$+G[\pm M-(\pm\tfrac{3}{2})]+\left[\frac{2D}{3}-(a-F)-GM\right][\pm M-(\pm\tfrac{1}{2})] \tag{4}$$

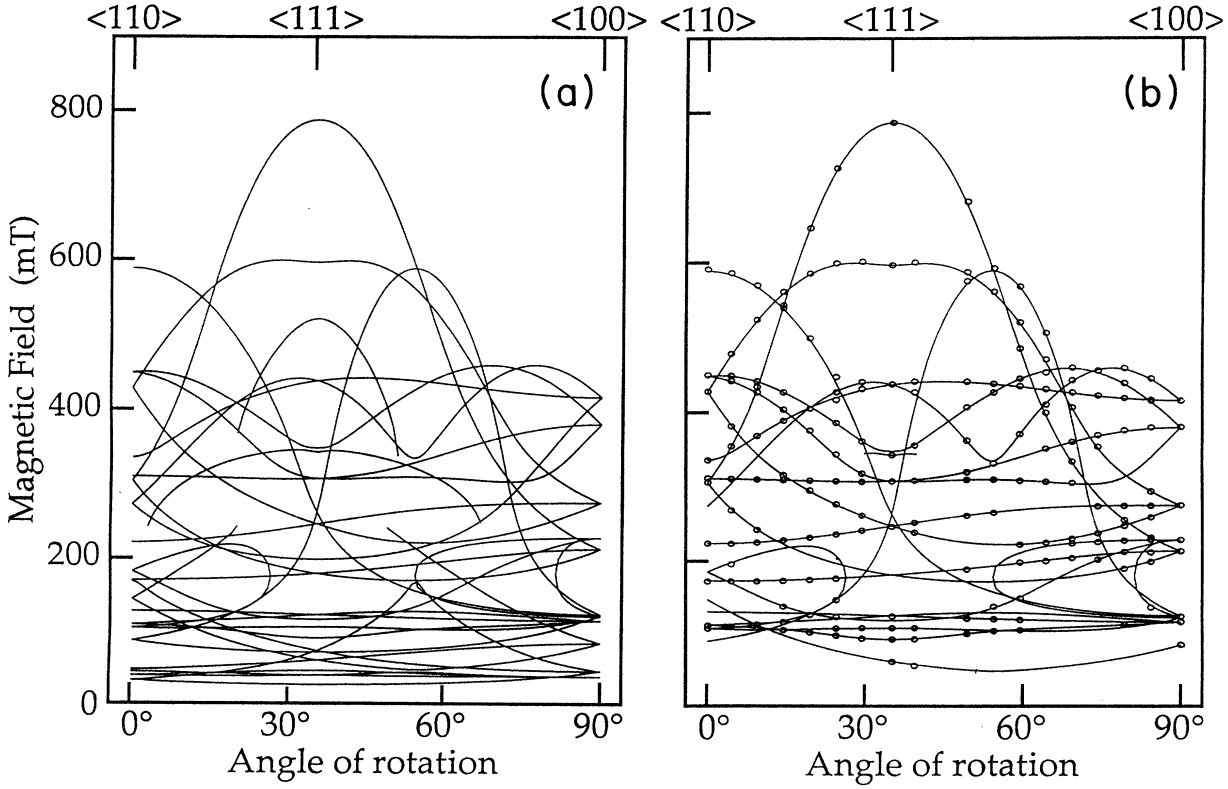

FIG. 3. Angular dependence of the fine-structure line positions of the (Cr^+-In^-) pair obtained at 9.526 GHz The magnetic field is rotated in a {110} plane. Left side: A plot of all possible fine structure transitions. Right side: The experimental data are plotted as open circles. The part of the calculated angular dependence for which experimental data exist is plotted as solid lines.

with $G=g_{\parallel}\mu_B B$, in which M refers to the dominant term in the spin function given by the diagonal part of the spin Hamiltonian (1). Since the cubic splitting parameter is very small compared with the Zeeman energy and the splitting parameter D in our case, the term $(20/9)a^2$ in the square root in Eq. (4), can be neglected in a first approximation the energy eigenvalues are determined by

$$E(M)=D(M^2-\tfrac{35}{12}) -[(a-F)/180](35M^4-475/2M^2+\tfrac{2835}{16}) +g_{\parallel}\mu_B BM\ , \quad (5)$$

which is identical with the contribution from the diagonal part of the spin Hamiltonian (1). Under this condition also the mixing between the wave functions $|\pm\frac{5}{2}\rangle$ and $|\pm\frac{1}{2}\rangle$ is negligible and M is a good quantum number. Therefore, we can only observe allowed transitions, i.e., $\Delta M=\pm 1$, in this particular direction. By identifying those transitions in the $\langle 111\rangle$ direction (which have the magnetic field parallel with the z direction) as those which do not show any forbidden hyperfine transitions discussed above, and using Eq. (5) we can calculate the values of the parameters D, $(a-F)$, and $g_{\parallel}$. The result is $g_{\parallel}=1.994$, $|D|=0.1077\ \text{cm}^{-1}$, and $|a-F|=0.0127\ \text{cm}^{-1}$, where the sign of $[D/(a-F)]$ is positive. In Fig. 4, the energy level scheme is drawn and the EPR transitions are indicated.

When the magnetic field is in another direction, the spin Hamiltonian is not diagonal even when neglecting the term proportional to a. One way to proceed is to apply perturbation theory but this is not possible in this

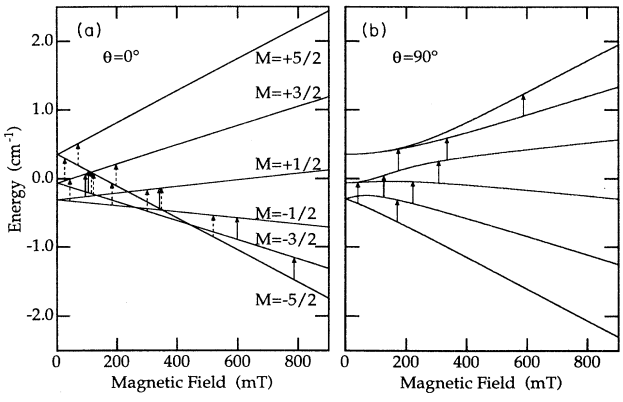

FIG. 4 Energy-level diagrams for the Cr^+-In^- defect for the magnetic field parallel (left) and perpendicular (right) to the trigonal axis. Possible EPR transitions at 9.526 GHz are indicated. For the parallel orientation only the allowed transitions (drawn as solid arrows) have a transition probability larger than zero. The forbidden transitions are drawn as dashed arrows. In the perpendicular positions all transitions have a transition probability larger than zero.

TABLE I. Spin Hamiltonian parameters of the (^{53}Cr-^{115}In) pair.

g values	Fine-structure parameters (10^{-4} cm^{-1})	Hyperfine-structure parameters (10^{-4} cm^{-1})
$g_{\parallel}=1.992\pm0.002$	$D=1075\pm5$	$A^{\mathrm{In}}=-7.2\pm0.1$
$g_{\perp}=2.003\pm0.004$	$\lvert D(^{53}\mathrm{Cr})-D(^{52}\mathrm{Cr})\rvert\leq0.1$	$B^{\mathrm{In}}=-3.0\pm0.1$
	$a-F=126\pm3$	$P_{\parallel}^{\mathrm{In}}=-2.2\pm0.2$
	$a=55\pm10$	$\lvert A^{\mathrm{Cr}}\rvert=10.5\pm0.1$
		$\lvert B^{\mathrm{Cr}}\rvert=10.7\pm0.1$

case since, as can be seen in Fig. 4, the zero-field and the Zeeman splittings in the magnetic-field region where the transitions occur are of the same order of magnitude. We therefore made a complete computer diagonalization of the SH. For different values of θ, the angle between the magnetic field and the z axis, we calculated the eigenvalues and eigenfunctions of the spin Hamiltonian as a function of the magnetic field and from this the position and intensity of the EPR lines were determined. We could then fit the calculated rotation pattern to the experimentally observed one and the result is indicated as solid lines in Fig. 3. The parameters of the SH found to give the best fit are summarized in Table I.

As previously mentioned, at $\theta=0$ only the allowed transitions, $\Delta M=\pm1$ (marked with solid arrows in Fig. 4) have measurable intensities, but when the sample is rotated away from this position also forbidden transitions, $\Delta M=\pm2,\pm3,\pm4,\pm5$ (marked with dashed arrows in Fig. 4) are observed. This is because M is no longer a good quantum number and therefore the eigenstates are mixed. When the magnetic field is perpendicular to the z axis the states are extremely mixed and all possible transitions have measurable intensities.

The sign of the parameters D, $(a-F)$, and a are more difficult to determine. If we reverse the sign, the energy-level scheme is turned upside down, i.e., there is no effect on the line position of the EPR spectrum. However, by studying the intensity of the different EPR transitions as a function of the temperature, the sign can in principle be determined. In our case, this was found to be difficult since the spectrum was strongly saturated at low temperatures. The measurement at higher temperatures and a measurement with a low modulation frequency (178 Hz) at 4.2 K indicate that the sign of the parameter D is positive.

In the Mn-B (Ref. 8) and Mn-Ga (Ref. 10) pairs a difference in the fine-structure parameter D has been observed for different isotopes of the acceptor. We therefore doped one sample with both ^{52}Cr and ^{53}Cr in order to investigate whether there is an isotope shift in D also for different TM isotopes in the TM-A pairs. However, no such shift was observed and we achieved a lower limit of a possible difference in D: $\Delta D=\lvert D(^{53}\mathrm{Cr})-D(^{52}\mathrm{Cr})\rvert\leq1\times10^{-5}$ cm^{-1}.

In order to explain the hyperfine structure of the spectrum, we have to include additional terms in the SH:

$$H=H_{FS}+H_Z+H_{\mathrm{Cr}}+H_{\mathrm{In}}\ , \tag{6}$$

$$H_{\mathrm{Cr}}=A^{\mathrm{Cr}}I_z^{\mathrm{Cr}}S_z+B^{\mathrm{Cr}}(I_x^{\mathrm{Cr}}S_x+I_y^{\mathrm{Cr}}S_y)\ , \tag{7}$$

$$\begin{aligned}H_{\mathrm{In}}=&A^{\mathrm{In}}I_z^{\mathrm{In}}S_z+B^{\mathrm{In}}(I_x^{\mathrm{In}}S_x+I_y^{\mathrm{In}}S_y)\\&+P_{\parallel}[(I_z^{\mathrm{In}})^2-1/3I^{\mathrm{In}}(I^{\mathrm{In}}+1)]\\&-g_N^{\mathrm{In}}\mu_N(B_xI_x^{\mathrm{In}}+B_yI_y^{\mathrm{In}}+B_zI_z^{\mathrm{In}})\ ,\end{aligned} \tag{8}$$

where H_{FS} and H_Z are described by Eqs. (2) and (3) and the symbols in Eqs. (7) and (8) have their usual meaning. Equation (7) is only important when doping with ^{53}Cr is performed. From this it is a straightforward procedure to determine the chromium hyperfine parameters. The terms reflecting the chromium quadrupole and nuclear Zeeman interaction were omitted because their influence is estimated to be very small and not measurable. Regardless, if the magnetic field is parallel with (see Fig. 2) or perpendicular to the trigonal axis, the ^{53}Cr hyperfine structure only shows the four allowed transitions, and therefore the A^{Cr} and B^{Cr} parameters are immediately deduced. These parameters are included in Table I.

The indium hyperfine interaction, on the other hand, is rather complicated. When the magnetic field is parallel with the trigonal axis only the ten allowed transitions

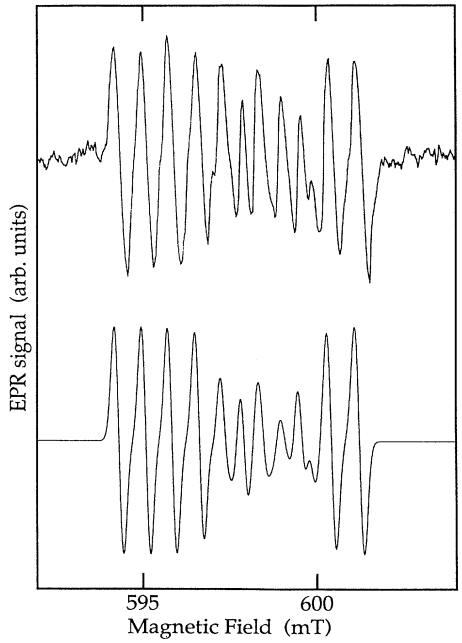

FIG. 5. Experimental (top) and calculated (bottom) indium hyperfine structure of the electronic spin transition $M=-\frac{3}{2}$ to $M=-\frac{1}{2}$ at $\theta=5°$.

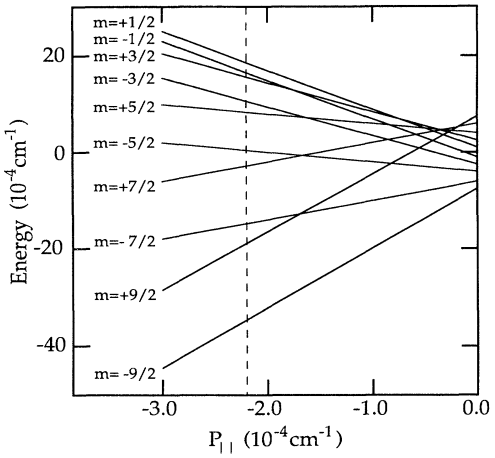

FIG. 6. Positions of the nuclear energy levels for the $M=-\frac{1}{2}$ state at $\theta=0°$ as a function of the quadrupole parameter $P_{\|}$. The indicated value is consistent with the experimental results.

occur (see Fig. 2). From the observed splitting of these lines the A^{In} parameter is determined. However, a rotation of the crystal a few degrees results in a completely different indium hyperfine pattern, with forbidden lines of large intensity. This means that we have an extensive mixing of the nuclear states which tells us that the quadrupole and/or the nuclear Zeeman interaction is of the same order of magnitude as the "normal" hyperfine interaction. In Fig. 5 the hyperfine structure for the $M=-\frac{3}{2}$ to $M=-\frac{1}{2}$ transition for $\theta=5°$ is shown. Here the structure is similar to the one at $\theta=0°$ (see Fig. 2) in the left and right part, but in the middle the intensity of the allowed transitions is decreased and new forbidden lines are observed. The transitions in the middle of the hyperfine pattern are between levels which have a small absolute value of the nuclear quantum number m. The fact that we observe forbidden lines in this part means that these nuclear states are mixed but the ones with high values of $|m|$ are not. This effect is mainly caused by the quadrupole interaction. In Fig. 6 the energy-level scheme of the $M=-\frac{1}{2}$ electronic state as a function of the quadrupole parameter $P_{\|}$ for $\theta=0°$ is shown. It can be seen in the figure that if $P_{\|}\approx-2.2\times10^{-4}$ cm^{-1}, the $m=+\frac{3}{2}$, $m=+\frac{1}{2}$ and $m=-\frac{1}{2}$ nuclear states are very close in energy. If there are matrix elements between these states they will mix extensively, since the mixing is proportional to $1/\delta$ (δ is here the distance between them). At $\theta=0°$ there are no matrix elements between them and thus no mixing and no forbidden hyperfine lines, but only a small rotation away from this position will introduce such matrix elements, and forbidden transitions appear.

In order to completely describe the hyperfine interaction we performed a computer diagonalization of the spin Hamiltonian described by Eqs. (2), (3), and (8). Since $S=\frac{5}{2}$ and $I=\frac{9}{2}$, this means diagonalizing a 60×60 matrix. We made this as a function of the angle θ and of the magnetic field and could, as described above, calculate the position and intensity of the EPR lines. In Fig. 5 the simulated spectrum is shown below the experimental one, and the determined indium hyperfine parameters are included in Table I. The g_N^{In} value, however, is not fitted, but instead we have used the value of the free atom, i.e., $g_N^{\mathrm{In}}=1.23$.

IV. DISCUSSION

From the hyperfine structure of the spectrum, it was concluded that it originates in a chromium-indium pair. Furthermore, the good agreement between the experimental points and the calculated positions of the EPR transitions shown in Fig. 3 is a convincing argument that the defect has trigonal symmetry and spin $\frac{5}{2}$. The model of the defect we propose is a nearest-neighbor $\mathrm{Cr}_i^{+}\mathrm{In}_s^{-}$ pair. The arguments for this interpretation are several. First, the In atom is incorporated into the silicon lattice as a substitutional impurity, while Cr is known to be an interstitial and can move around in the crystal, even at room temperature, until it is trapped next to an indium atom. The attractive force between the two atoms is the Coulomb attraction. Second, the In^{-} ion has a closed shell and does not contribute to the spin of the defect. Cr^{+}, on the other hand has a $^6S_{5/2}$ configuration which means that the spin of the defect will be $\frac{5}{2}$, in agreement with the experimentally determined value. Third, the trigonal symmetry observed is consistent with the suggested model of a Cr ion on a nearest interstitial position of a substitutional In.

Another point which favors our interpretation of the charge state is the fact that the Cr-In-pair spectrum is only observed during illumination of the sample. In analogy with the other chromium-acceptor pairs,[11,12] we expect the Cr-In pair to introduce a donor level in the forbidden energy gap. Since our sample is prepared from p-type material the charge state in darkness should be $(\mathrm{Cr}\text{-}\mathrm{In})^{+}$, i.e., we have to fill the level with an electron to achieve the neutral charge state, which is in agreement with the experimental fact that we have to illuminate the sample in order to observe the EPR spectrum.

It is of interest to understand why the $(\mathrm{Fe}^{+}\text{-}A^{-})$ pairs show metastable properties while the $(\mathrm{Mn}^{2+}\text{-}A^{-})$ pairs do not.[9] One reason could be that the extra charge of the Mn^{2+} ion increases the Coulomb interaction which would favor the nearest-neighbor position. Another reason might be the different electronic configurations, with the ground state $^4F_{3/2}$ for Fe^{+} and $^6S_{5/2}$ for Mn^{2+} and the different lattice relaxation produced by the different TM ions. The Cr-A pairs have the same charge state as the Fe-A pairs, and the same electronic configuration as the Mn-A defects. The fact that only the nearest-neighbor position is observed for all Cr-A pairs suggests that the electronic configuration plays an important role in the case of metastability. An argument against this conclusion might be the previously discussed fact that the Cr-In defect is only observed if the sample is illuminated. This means that the defect is in the $(\mathrm{Cr}^{2+}\text{-}\mathrm{In}^{-})$ charge state during cooling, and if the temperature at the EPR measurements is too low for the Cr atom to jump to the other position, the charge state might still be the dominant reason for the lack of metastability. It is

interesting to mention that if we had the light on during cooling no additional EPR spectrum could be detected and there was no significant change in intensity in the observed spectrum.

V. CONCLUSIONS

A new EPR spectrum is observed in silicon doped with indium and chromium. From the hyperfine interactions, the corresponding defect is identified as a Cr-In pair. From the complicated fine structure of the spectrum, the defect is determined to have trigonal symmetry and spin equal to $\frac{5}{2}$. The proposed model is a (Cr_i^+-In_s^-), where the electronic properties originate in the $^6S_{5/2}$ ground state of the $3d^5$ configuration of the Cr^+ ion. The indium hyperfine structure is also complicated and the quadrupole interaction is found to be an important part of the hyperfine interaction.

ACKNOWLEDGMENTS

This work was supported by the Swedish National Science Research Council and the Swedish Board for Technical Development.

[1]G. W. Ludwig and H. H. Woodbury, in *Solid State Physics,* edited by F. Seitz and D. Turnbull (Academic, New York, 1962), Vol. 13, p. 223.

[2]A. Chantre and D. Bois, Phys. Rev. B **31**, 7979 (1985).

[3]J. J. van Kooten, G. A. Weller, and C. A. J. Ammerlaan, Phys. Rev. B **30**, 4564 (1984).

[4]W. Gehlhoff, K. Irmscher, and J. Kreissl, in *New Developments in Semiconductor Physics,* edited by G. Ferenczi and F. Beleznay, Lecture Notes in Physics Vol. 301 (Springer-Verlag, Berlin, 1988), p. 262.

[5]A. Chantre and L. C. Kimerling, in *Materials Science Forum,* edited by H. J. von Bardeleben (Trans Tech, Aedermannsdorf, 1986), Vols. 10–12, p. 387.

[6]P. Omling, P. Emanuelsson, W. Gehlhoff, and H. G. Grimmeiss, Solid State Commun. **70**, 807 (1989).

[7]W. Gehlhoff, P. Emanuelsson, P. Omling, and H. G. Grimmeiss, Phys. Rev. B **41**, 8560 (1990).

[8]J. Kreissl and W. Gehlhoff, Phys. Status Solidi B **112**, 695 (1982).

[9]J. Kreissl, W. Gehlhoff, P. Omling, and P. Emanuelsson, Phys. Rev. B **42**, 1731 (1990).

[10]J. Kreissl, K. Irmscher, W. Gehlhoff, P. Omling, and P. Emanuelsson, Phys. Rev. B **44**, 3678 (1991).

[11]H. Lemke, Phys. Status Solidi A **75**, K49 (1983).

[12]H. Lemke, Phys. Status Solidi A **76**, 223 (1983).

[13]H. Feichtinger, J. Oswald, R. Czaputa, P. Vogl, and K. Wünstel, in *Proceedings of the 13th International Conference on Defects in Semiconductors,* edited by L. C. Kimerling and J. M. Parsey, Jr. (The Metallurgical Society of AIME, Warrendale, PA, 1985), p. 855.

[14]H. Conzelmann, K. Graff, and E. R. Weber, Appl. Phys. A **30**, 169 (1983).

[15]H. Conzelmann, Appl. Phys. A **42**, 1 (1987).

[16]U. Reisloehner and W. Witthuhn, Mater. Sci. Forum **65-66**, 281 (1990).